



Contents lists available at ScienceDirect

Earth and Planetary Science Letters

www.elsevier.com/locate/epsl



Unusually deep Bonin earthquake of 30 May 2015: A precursory signal to slab penetration?

Masayuki Obayashi^{a,*}, Yoshio Fukao^b, Junko Yoshimitsu^a

^a Department of Deep Earth Structure and Dynamics Research, Japan Agency for Marine–Earth Science and Technology, Natsushima-cho 2-15, Yokosuka, Kanagawa, 237-0061, Japan

^b Research and Development Center for Earthquake and Tsunami, Japan Agency for Marine–Earth Science and Technology, Yokohama, Kanagawa, 236-0001, Japan

ARTICLE INFO

Article history:

Received 26 August 2016
Received in revised form 7 November 2016
Accepted 9 November 2016
Available online xxxx
Editor: P. Shearer

Keywords:

deep earthquake
stagnant slab
slab penetration
660-km discontinuity

ABSTRACT

An M7.9 earthquake occurred on 30 May 2015 at an unusual depth of 680 km downward and away from the well-defined Wadati–Benioff (WB) zone of the southern Bonin arc. To the north (northern Bonin), the subducted slab is stagnant above the upper–lower mantle boundary at 660-km depth, where the WB zone bends forward to sub-horizontal. To the south (northern Mariana), it penetrates the boundary, where the WB zone extends near-vertically down to the boundary. Thus, the southern Bonin slab can be regarded as being in a transitional state from slab stagnation to penetration. The transition is shown to happen rapidly within the northern half of the southern Bonin slab where the heel part of the shoe-like configured stagnant slab hits the significantly depressed 660-km discontinuity. The mainshock and aftershocks took place in this heel part where they are sub-vertically aligned in approximate parallel to their maximum compressional axes. Here, the dips of the compressional axes of WB zone earthquakes change rapidly across the thickness of the slab from the eastern to western side and along the strike of the slab from the northern to southern side, suggesting rapid switching of the downdip compression axis in the shoe-shaped slab. Elastic deformation associated with the WB zone seismicity is calculated by viewing it as an integral part of the slab deformation process. With this deformation, the heel part is deepened relative to the arch part and is compressed sub-vertically and stretched sub-horizontally, a tendency consistent with the idea of progressive decent of the heel part in which near-vertical compressional stress is progressively accumulated to generate isolated shocks like the 2015 event and eventually to initiate slab penetration.

© 2016 Elsevier B.V. All rights reserved.

1. Introduction

The earthquake occurred on 30 May 2015 at unusual depth of 680 km was the 5th largest of earthquakes below 300 km since 1960 (Houston, 2007). This event, referred to as the Bonin super deep (BSD) shock, is unique not only because of its considerable depth and magnitude (global CMT; <http://www.globalcmt.org>; Dziewonski et al., 1981; Ekström et al., 2012) but also because of its location in the subducting Pacific slab (Ye et al., 2016; Takemura et al., 2016). Fig. 1A shows the vertical cross-section of a three-dimensional P-wave tomography model, GAP_P4 (Obayashi et al., 2013; Fukao and Obayashi, 2013) along the east–west profile through the hypocenter (red dot in Fig. 1). The cold subducting Pacific slab is imaged as fast anomalies (in blue). From the surface down to the transition zone the slab sub-vertically dips and then

sharply bends to sub-horizontal near the 660-km discontinuity. The hypocentral distribution of deep shocks in the past (Engdahl et al., 1998) defines the WB zone, which delineates the cold core of the subducting slab. Note that the WB zone between 450 and 550 km depths also kinks where the tomographically imaged slab bends. An event isolated from the WB zone is the 6.7 magnitude, 547.5-km-depth event on 4 July 1982 (Lundgren and Giardini, 1994) (green dot in Fig. 1A). This event occurred several hundreds of kilometers west in front of the main WB zone; however, it was still located near the core of the horizontally deflected part of the slab. An even more isolated event was the BSD shock that was located downwards and away from the WB zone. Its location corresponds to the heel portion of the bent slab, the appearance of which is similar to a shoe in the cross-sectional view.

Although the focal depth exceeds the nominal depth of the 660-km discontinuity, the actual depth of the 660-km discontinuity can vary significantly depending on the thermal and compositional environment because of its phase boundary nature (Ito and Takahashi, 1989; Bina and Helffrich, 1994). The boundary depth

* Corresponding author.

E-mail address: obayashi@jamstec.go.jp (M. Obayashi).

<http://dx.doi.org/10.1016/j.epsl.2016.11.019>

0012-821X/© 2016 Elsevier B.V. All rights reserved.

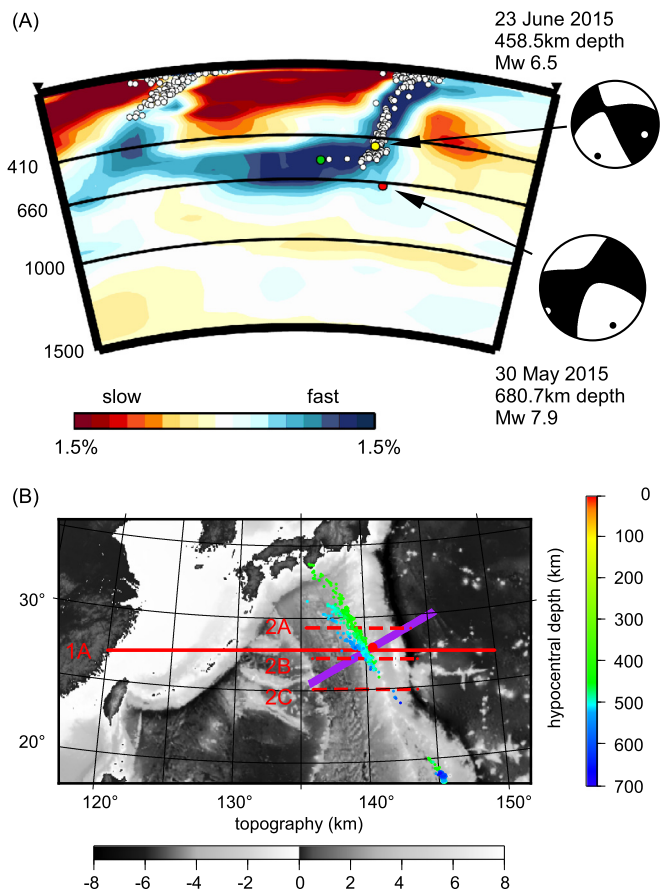


Fig. 1. Location of the BSD shock. (A) The east–west cross-section (solid red line in (B)) of the GAP_P4 model. White dots indicate the hypocenters (Engdahl et al., 1998) within a band 50 km wide on both sides of the section plane. The focal mechanisms of the BSD shock and a subsequent earthquake on 23 June 2015 are projected onto the section plane. Black and white dots on the focal mechanism indicate the maximum and minimum compression directions, respectively. (B) Geographical location of the BSD shock (red dot). The hypocenters below 400 km are shown by colors varying with depth. The three broken red lines and a thick purple line are referred to in Figs. 3 and 5, respectively. (For interpretation of the references to color in this figure legend, the reader is referred to the web version of this article.)

in this region has been studied using S-to-P converted waves (Vidale and Benz, 1992; Wicks and Richards, 1993; Collier and Helffrich, 1997; Castle and Creager, 1998). The 660-km discontinuity is depressed by 35 ± 17 km (Castle and Creager, 1998); therefore, the hypocenter is in close proximity to the boundary, although it is difficult to judge whether the hypocenter lies above or below the depressed boundary owing to the lack of nearby conversion points and uncertainties in the hypocentral and conversion depths. A recent study using P-to-S converted waves reported that the 660-km discontinuity is at 690 km depth with up to ~ 15 km variability, immediately below the BSD shock (Porritt and Yoshioka, 2016). Previous seismic tomography models have consistently shown morphological changes of subducting slabs from Izu–Bonin where the slab is stagnant at the base of the upper mantle to Mariana where the slab is penetrating vertically into the lower mantle (e.g. van der Hilst et al., 1991; Fukao et al., 1992; van der Hilst and Seno, 1993; Miller et al., 2005). The BSD shock was located in the transitional region from slab stagnation to penetration. In this paper we consider the implications for the 2015 event by integrating our recent tomographic images, hypocentral distribution and focal mechanisms of the mainshock and aftershocks and the strain field around the hypocenter induced by WB zone seismicity.

2. Slab morphology from Bonin to Mariana

Fig. 2 shows a morphological change of the slab from northern Bonin (A–D), southern Bonin (E–H) to northern Mariana (I–L) based on the GAP_P4 model. In northern Bonin, the slab bends horizontally along the 660-km discontinuity, and its bending becomes increasingly sharp towards the south (A→D) by a progressive deepening of the bending portion. In northern Mariana, on the other hand, the slab is penetrating and the penetrated mass increases towards the south (I→L) (Fukao and Obayashi, 2013). The images in southern Bonin are understood to be those at the transitional stage from slab stagnation to penetration (E→H). Figs. 3A, 3B and 3C show slab images between the two adjacent sections C and D, E and F, and G and H, respectively, where the seismicity and focal mechanisms in the northern and southern sections are superposed in different colors. The resolution tests indicate that each of the targeted blocks near the 660-km discontinuity is reasonably resolved (Appendix A in Supplementary material). At the C→D stage (Fig. 3A) the heel part of the stagnant slab is rapidly deepening as it goes southward, although it does not yet reach the 660-km discontinuity. At the E→F stage (Fig. 3B) the heel part of the stagnant slab hits the 660-km discontinuity and depresses the 660-km phase boundary (Porritt and Yoshioka, 2016). This depression generates near-vertical compressional stresses in the heel portion just above the depressed boundary (Yoshioka et al., 1997; Bina, 1997; Bina et al., 2001). We interpret the BSD shock as a consequence of this stress environment. The horizontally deflected part of the slab becomes progressively decoupled from the rest. The rest behaves as a coherent body of near-vertical, slightly buckled slab (Alpert et al., 2010), which begins to penetrate the 660-km discontinuity at the G→H stage (Fig. 3C). Deep shocks at this stage are consistently down-dip compressional.

3. Aftershocks

The slab at the E→F stage (Fig. 3B) is therefore the mature stagnant slab in a transitional state to penetrating slab. The BSD shock and its aftershocks may be regarded as the forerunners of WB zone earthquakes at greatest depths in the near-vertically downgoing slab continuing all the way from the surface, as will be discussed below. Only five aftershocks were reported by the USGS National Earthquake Information Center (USGS-NEIC) (Japan Meteorological Agency (JMA) reported four aftershocks except for the first one). The first three aftershocks occurred within 2 h of the BSD shock and the remaining two, including the largest event with Mb 4.9 (2 June 2015), occurred 3 to 5 days after the BSD shock. We simultaneously relocated the mainshock and aftershocks using the first arrival data collected by USGS-NEIC. The relocation method incorporates absolute travel-time residuals and differential travel-time residuals between different events at the same stations, referred to as double differences (Waldhauser and Ellsworth, 2000), to constrain their relative locations. The travel time residuals were calculated with respect to the GAP_P4 model. The result is shown with estimated errors in Fig. 4A compared to the USGS-NEIC and JMA hypocenters. The depth of the BSD shock was relocated to 683.6 km that is closer to the JMA determination. The relocated aftershocks became closer to the mainshock and to each other than the original USGS-NEIC determinations. Unlike the subevents of the mainshock (Ye et al., 2016), the aftershocks do not lie on either of the nodal planes of the mainshock but rather extend in deeper directions.

Fig. 4B shows the first motion polarities of the largest aftershock. The up-or-down initial motions of this aftershock were visually evaluated on the vertical P-wave records of the IRIS broadband network and the Japanese high-sensitivity seismograph net-

Download English Version:

<https://daneshyari.com/en/article/5780140>

Download Persian Version:

<https://daneshyari.com/article/5780140>

[Daneshyari.com](https://daneshyari.com)